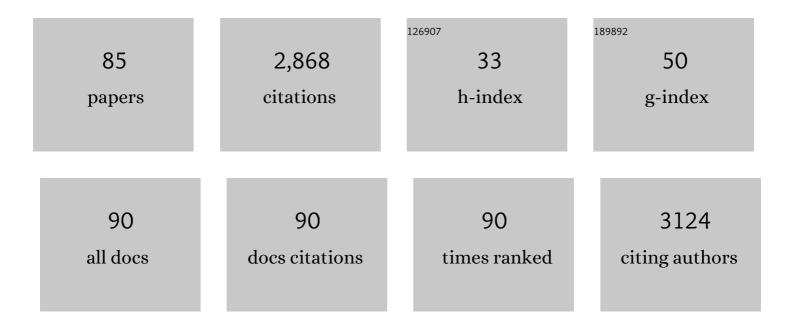
Oleksandr Polonskyi

List of Publications by Year in descending order

Source: https://exaly.com/author-pdf/6316/publications.pdf Version: 2024-02-01



#	Article	IF	CITATIONS
1	Impact of argon flow and pressure on the trapping behavior of nanoparticles inside a gas aggregation source. Plasma Processes and Polymers, 2022, 19, e2100125.	3.0	6
2	In Situ Monitoring of Scale Effects on Phase Selection and Plasmonic Shifts during the Growth of AgCu Alloy Nanostructures for Anticounterfeiting Applications. ACS Applied Nano Materials, 2022, 5, 3832-3842.	5.0	7
3	Real-time insight into nanostructure evolution during the rapid formation of ultra-thin gold layers on polymers. Nanoscale Horizons, 2021, 6, 132-138.	8.0	24
4	Revealing the growth of copper on polystyrene-block-poly(ethylene oxide) diblock copolymer thin films with in situ GISAXS. Nanoscale, 2021, 13, 10555-10565.	5.6	11
5	Selective Silver Nanocluster Metallization on Conjugated Diblock Copolymer Templates for Sensing and Photovoltaic Applications. ACS Applied Nano Materials, 2021, 4, 4245-4255.	5.0	14
6	Hierarchical colloid-based lithography for wettability tuning of semiconductor surfaces. Journal of Vacuum Science and Technology A: Vacuum, Surfaces and Films, 2021, 39, .	2.1	5
7	Polymethylmethacrylate wettability change spatially correlates with self-organized streamer microdischarge patterns in dielectric barrier discharge plasmas. Journal of Vacuum Science and Technology A: Vacuum, Surfaces and Films, 2021, 39, .	2.1	8
8	Enhancing composition control of alloy nanoparticles from gas aggregation source by in operando optical emission spectroscopy. Plasma Processes and Polymers, 2021, 18, 2000208.	3.0	12
9	Correlating Optical Reflectance with the Topology of Aluminum Nanocluster Layers Growing on Partially Conjugated Diblock Copolymer Templates. ACS Applied Materials & Interfaces, 2021, 13, 56663-56673.	8.0	9
10	Precise localization of DBD plasma streamers using topographically patterned insulators for maskless structural and chemical modification of surfaces. Applied Physics Letters, 2021, 119, 211601.	3.3	7
11	Nucleation and Growth of Magnetronâ€Sputtered Ag Nanoparticles as Witnessed by Timeâ€Resolved Small Angle Xâ€Ray Scattering. Particle and Particle Systems Characterization, 2020, 37, 1900436.	2.3	30
12	Following in Situ the Deposition of Gold Electrodes on Low Band Gap Polymer Films. ACS Applied Materials & Interfaces, 2020, 12, 1132-1141.	8.0	10
13	PdO nanoparticles decorated TiO2 film with enhanced photocatalytic and self-cleaning properties. Materials Today Chemistry, 2020, 16, 100251.	3.5	22
14	Photodeposition of Au Nanoclusters for Enhanced Photocatalytic Dye Degradation over TiO ₂ Thin Film. ACS Applied Materials & Interfaces, 2020, 12, 14983-14992.	8.0	75
15	Low-Temperature Solution Synthesis of Au-Modified ZnO Nanowires for Highly Efficient Hydrogen Nanosensors. ACS Applied Materials & amp; Interfaces, 2019, 11, 32115-32126.	8.0	49
16	Antibacterial, highly hydrophobic and semi transparent Ag/plasma polymer nanocomposite coating on cotton fabric obtained by plasma based co-deposition. Cellulose, 2019, 26, 8877-8894.	4.9	34
17	Durability of resin bonding to zirconia ceramic after contamination and the use of various cleaning methods. Dental Materials, 2019, 35, 1388-1396.	3.5	22
18	Correlating Nanostructure, Optical and Electronic Properties of Nanogranular Silver Layers during Polymer-Template-Assisted Sputter Deposition. ACS Applied Materials & Interfaces, 2019, 11, 29416-29426.	8.0	37

OLEKSANDR POLONSKYI

#	Article	IF	CITATIONS
19	The evolution of Ag nanoparticles inside a gas aggregation cluster source. Plasma Processes and Polymers, 2019, 16, 1900079.	3.0	20
20	Wet-Chemical Assembly of 2D Nanomaterials into Lightweight, Microtube-Shaped, and Macroscopic 3D Networks. ACS Applied Materials & Interfaces, 2019, 11, 44652-44663.	8.0	30
21	Pathways to Tailor Photocatalytic Performance of TiO2 Thin Films Deposited by Reactive Magnetron Sputtering. Materials, 2019, 12, 2840.	2.9	59
22	Ag Nanoparticles Decorated TiO 2 Thin Films with Enhanced Photocatalytic Activity. Physica Status Solidi (A) Applications and Materials Science, 2019, 216, 1800898.	1.8	15
23	Superhydrophobic 3D Porous PTFE/TiO ₂ Hybrid Structures. Advanced Materials Interfaces, 2019, 6, 1801967.	3.7	19
24	Effect of noble metal functionalization and film thickness on sensing properties of sprayed TiO2 ultra-thin films. Sensors and Actuators A: Physical, 2019, 293, 242-258.	4.1	19
25	Cauliflower-like CeO ₂ –TiO ₂ hybrid nanostructures with extreme photocatalytic and self-cleaning properties. Nanoscale, 2019, 11, 9840-9844.	5.6	24
26	Superhydrophobic Surfaces: Superhydrophobic 3D Porous PTFE/TiO2 Hybrid Structures (Adv. Mater.) Tj ETQq0 0	0	verlock 10 Tf
27	A comparative study of photocatalysis on highly active columnar TiO2 nanostructures in-air and in-solution. Solar Energy Materials and Solar Cells, 2018, 178, 170-178.	6.2	59
28	(CuO-Cu2O)/ZnO:Al heterojunctions for volatile organic compound detection. Sensors and Actuators B: Chemical, 2018, 255, 1362-1375.	7.8	47
29	Tuning doping and surface functionalization of columnar oxide films for volatile organic compound sensing: experiments and theory. Journal of Materials Chemistry A, 2018, 6, 23669-23682.	10.3	36
30	Magnetron-sputtered copper nanoparticles: lost in gas aggregation and found by <i>in situ</i> X-ray scattering. Nanoscale, 2018, 10, 18275-18281.	5.6	46
31	Plasma based formation and deposition of metal and metal oxide nanoparticles using a gas aggregation source. European Physical Journal D, 2018, 72, 1.	1.3	29
32	PdO/PdO ₂ functionalized ZnO : Pd films for lower operating temperature H ₂ gas sensing. Nanoscale, 2018, 10, 14107-14127.	5.6	114
33	Role of UV Plasmonics in the Photocatalytic Performance of TiO ₂ Decorated with Aluminum Nanoparticles. ACS Applied Nano Materials, 2018, 1, 3760-3764.	5.0	35
34	Ultra-thin TiO2 films by atomic layer deposition and surface functionalization with Au nanodots for sensing applications. Materials Science in Semiconductor Processing, 2018, 87, 44-53.	4.0	30
35	Efficacy of Plasma Treatment for Decontaminating Zirconia. Journal of Adhesive Dentistry, 2018, 20, 289-297.	0.5	17
36	Role of Sputter Deposition Rate in Tailoring Nanogranular Gold Structures on Polymer Surfaces. ACS Applied Materials & Interfaces, 2017, 9, 5629-5637.	8.0	64

OLEKSANDR POLONSKYI

#	Article	IF	CITATIONS
37	Localized Synthesis of Iron Oxide Nanowires and Fabrication of High Performance Nanosensors Based on a Single Fe ₂ O ₃ Nanowire. Small, 2017, 13, 1602868.	10.0	111
38	Single target sputter deposition of alloy nanoparticles with adjustable composition via a gas aggregation cluster source. Nanotechnology, 2017, 28, 175703.	2.6	52
39	Extreme tuning of wetting on 1D nanostructures: from a superhydrophilic to a perfect hydrophobic surface. Nanoscale, 2017, 9, 14814-14819.	5.6	12
40	Light-induced Conductance Switching in Photomechanically Active Carbon Nanotube-Polymer Composites. Scientific Reports, 2017, 7, 9648.	3.3	11
41	Single-step generation of metal-plasma polymer multicore@shell nanoparticles from the gas phase. Scientific Reports, 2017, 7, 8514.	3.3	27
42	Modification of a metal nanoparticle beam by a hollow electrode discharge. Journal of Vacuum Science and Technology A: Vacuum, Surfaces and Films, 2016, 34, 021301.	2.1	2
43	Non-planar nanoscale p–p heterojunctions formation in Zn Cu1O nanocrystals by mixed phases for enhanced sensors. Sensors and Actuators B: Chemical, 2016, 230, 832-843.	7.8	70
44	Antibacterial nanocomposite coatings produced by means of gas aggregation source of silver nanoparticles. Surface and Coatings Technology, 2016, 294, 225-230.	4.8	52
45	Multifunctional device based on ZnO:Fe nanostructured films with enhanced UV and ultra-fast ethanol vapour sensing. Materials Science in Semiconductor Processing, 2016, 49, 20-33.	4.0	73
46	Enhanced ethanol vapour sensing performances of copper oxide nanocrystals with mixed phases. Sensors and Actuators B: Chemical, 2016, 224, 434-448.	7.8	140
47	Real-Time Monitoring of Morphology and Optical Properties during Sputter Deposition for Tailoring Metal–Polymer Interfaces. ACS Applied Materials & Interfaces, 2015, 7, 13547-13556.	8.0	113
48	Stable production of TiO _x nanoparticles with narrow size distribution by reactive pulsed dc magnetron sputtering. Journal Physics D: Applied Physics, 2015, 48, 035501.	2.8	24
49	Nylon-sputtered plasma polymer particles produced by a semi-hollow cathode gas aggregation source. Vacuum, 2015, 111, 124-130.	3.5	13
50	Hydrophobic and super-hydrophobic coatings based on nanoparticles overcoated by fluorocarbon plasma polymer. Vacuum, 2014, 100, 57-60.	3.5	48
51	Fabrication of Cu nanoclusters and their use for production of Cu/plasma polymer nanocomposite thin films. Thin Solid Films, 2014, 550, 46-52.	1.8	41
52	Photovoltage method for the research of CdS and ZnO nanoparticles and hybrid MEH-PPV/nanoparticle structures. Journal of Nanoparticle Research, 2014, 16, 1.	1.9	3
53	Deposition of Al nanoparticles and their nanocomposites using a gas aggregation cluster source. Journal of Materials Science, 2014, 49, 3352-3360.	3.7	28
54	Deposition and characterization of Pt nanocluster films by means of gas aggregation cluster source. Thin Solid Films, 2014, 571, 13-17.	1.8	19

#	Article	IF	CITATIONS
55	Versatile Growth of Freestanding Orthorhombic α-Molybdenum Trioxide Nano- and Microstructures by Rapid Thermal Processing for Gas Nanosensors. Journal of Physical Chemistry C, 2014, 118, 15068-15078.	3.1	114
56	Huge increase in gas phase nanoparticle generation by pulsed direct current sputtering in a reactive gas admixture. Applied Physics Letters, 2013, 103, .	3.3	35
57	Gas barrier properties of hydrogenated amorphous carbon films coated on polyethylene terephthalate by plasma polymerization in argon/n-hexane gas mixture. Thin Solid Films, 2013, 540, 65-68.	1.8	10
58	Characterization of nanoparticle flow produced by gas aggregation source. Vacuum, 2013, 96, 32-38.	3.5	48
59	Role of oxygen admixture in stabilizing TiO x nanoparticle deposition from a gas aggregation source. Journal of Nanoparticle Research, 2013, 15, 1.	1.9	21
60	Analysis of aerodynamics and charging of nanoparticles in the gas aggregation source based on a planar magnetron. , 2012, , .		0
61	Influence of reactive gas admixture on transition metal cluster nucleation in a gas aggregation cluster source. Journal of Applied Physics, 2012, 112, .	2.5	44
62	Nylon-sputtered nanoparticles: fabrication and basic properties. Journal Physics D: Applied Physics, 2012, 45, 495301.	2.8	32
63	Nanocomposite coatings of Ti/C:H plasma polymer particles providing a surface with variable nanoroughness. Surface and Coatings Technology, 2012, 206, 4335-4342.	4.8	25
64	Effect of sterilization procedures on properties of plasma polymers relevant to biomedical applications. Thin Solid Films, 2012, 520, 7115-7124.	1.8	16
65	Nanocomposite and nanostructured films with plasma polymer matrix. Surface and Coatings Technology, 2012, 211, 127-137.	4.8	24
66	Control of Wettability of Plasma Polymers by Application of Ti Nano lusters. Plasma Processes and Polymers, 2012, 9, 180-187.	3.0	33
67	Deposition of Fluorocarbon Nanoclusters by Gas Aggregation Cluster Source. Plasma Processes and Polymers, 2012, 9, 390-397.	3.0	19
68	Deposition of Pt nanoclusters by means of gas aggregation cluster source. Materials Letters, 2012, 79, 229-231.	2.6	40
69	Nanocomposite metal/plasma polymer films prepared by means of gas aggregation cluster source. Thin Solid Films, 2012, 520, 4155-4162.	1.8	57
70	Structure and Composition of Titanium Nanocluster Films Prepared by a Gas Aggregation Cluster Source. Journal of Physical Chemistry C, 2011, 115, 20937-20944.	3.1	43
71	Deposition of amino-rich coatings by RF magnetron sputtering of Nylon: In-situ characterization of the deposition process. Surface and Coatings Technology, 2011, 205, S558-S561.	4.8	6
72	Nanostructured thin films prepared from cluster beams. Surface and Coatings Technology, 2011, 205, S42-S47.	4.8	33

#	Article	IF	CITATIONS
73	Aging of nanocluster Ti/TiOx films prepared by means of gas aggregation cluster source. Surface and Coatings Technology, 2011, 205, S48-S52.	4.8	13
74	Deposition of amino-rich coatings by RF magnetron sputtering of Nylon: Investigation of their properties related to biomedical applications. Surface and Coatings Technology, 2011, 205, S529-S533.	4.8	7
75	Morphology of Titanium Nanocluster Films Prepared by Gas Aggregation Cluster Source. Plasma Processes and Polymers, 2011, 8, 640-650.	3.0	41
76	Nanocomposite gold/poly(ethylene oxide)-like plasma polymers prepared by plasma-assisted vacuum evaporation and magnetron sputtering. Surface and Coatings Technology, 2011, 205, 2830-2837.	4.8	5
77	Deposition of nanostructured fluorocarbon plasma polymer films by RF magnetron sputtering of polytetrafluoroethylene. Thin Solid Films, 2011, 519, 6426-6431.	1.8	38
78	Structured Ti/Hydrocarbon Plasma Polymer Nanocomposites Produced By Magnetron Sputtering with Glancing Angle Deposition. Plasma Processes and Polymers, 2010, 7, 25-32.	3.0	30
79	Poly(ethylene oxide)â€like Plasma Polymers Produced by Plasmaâ€Assisted Vacuum Evaporation. Plasma Processes and Polymers, 2010, 7, 445-458.	3.0	56
80	Superâ€Hydrophobic Coatings Prepared by RF Magnetron Sputtering of PTFE. Plasma Processes and Polymers, 2010, 7, 544-551.	3.0	86
81	PEO-Like Coatings Prepared by Plasma-Based Techniques. Plasma Processes and Polymers, 2009, 6, S21-S24.	3.0	7
82	NMR Study of Polyethylene‣ike Plasma Polymer Films. Plasma Processes and Polymers, 2009, 6, S362.	3.0	5
83	In Situ Diagnostics of RF Magnetron Sputtering of Nylon. Plasma Processes and Polymers, 2009, 6, S803.	3.0	22
84	Vacuum Thermal Degradation of Poly(ethylene oxide). Journal of Physical Chemistry B, 2009, 113, 2984-2989.	2.6	53
85	Covalent Attachment and Bioactivity of Horseradish Peroxidase on Plasmaâ€Polymerized Hexane Coatings. Plasma Processes and Polymers, 2008, 5, 727-736.	3.0	20